

Signed Distance Function Computation from an Implicit Surface

Pierre-Alain Fayolle
 Computer Graphics Laboratory, University of Aizu,
 Aizu-Wakamatsu, Japan,
 fayolle@u-aizu.ac.jp

Abstract

We describe in this short note a technique to convert an implicit surface into a Signed Distance Function (SDF) while exactly preserving the zero level-set of the implicit. The proposed approach relies on embedding the input implicit in the final layer of a neural network, which is trained to minimize a loss function characterizing the SDF.

1 Introduction

We consider in this note the problem of computing the Signed Distance Function (SDF) to an implicit surface. Let a surface S be defined as the zero level-set of a function f , $S = \{\mathbf{x} \in \mathbb{R}^3 : f(\mathbf{x}) = 0\}$. We propose a method for computing the signed distance to S :

$$d(\mathbf{x}) = \pm \text{dist}(\mathbf{x}, S) = \pm \min_{\mathbf{y} \in S} |\mathbf{x} - \mathbf{y}|, \quad (1)$$

while preserving exactly the zero level-set of f . W.l.o.g we assume that $d > 0$ inside the domain bounded by S and that $d < 0$ outside.

In the literature on level-set methods, techniques for computing the SDF d from f are called re-initialization methods [23, 14]. One considers the problem:

$$\partial g(\mathbf{x}, t) / \partial t + (1 - |\nabla_{\mathbf{x}} g(\mathbf{x}, t)|) = 0 \quad g(\mathbf{x}, 0) = f(\mathbf{x}) \quad (2)$$

and solves it to steady-state. Typically, (2) is solved by discretizing the time derivative with explicit or implicit Euler, and the spatial derivative by finite difference [23]. Another popular approach for computing (1) is the

Fast Marching Method [19].

In each case, the approach relies on computing a regular grid for the domain, and sampling functions and derivatives on this grid. Thus the zero level-set of g does not correspond exactly to the zero level-set of f .

On the other hand, the method described here preserves exactly the zero level-set of f . It does so by computing the signed distance $d(\mathbf{x}; \boldsymbol{\theta})$ as $f(\mathbf{x})g(\mathbf{x}; \boldsymbol{\theta})$, where $g(\cdot)$ is a parametric function whose parameters $\boldsymbol{\theta}$ are fitted such that d corresponds to the distance function.

2 Related work

Distance to an implicit surface The simplest method for turning f into a SDF consists in meshing the zero level-set S , for example with the Marching Cubes algorithm [13], and then to compute the distance to the polygonal mesh. Typically accelerating data-structures, such as a Kd-Tree or a Bounding Volume Hierarchy (BVH), are used for practical computations.

Re-initialization (or re-distancing) a scalar field f sampled on a grid is a common operation in level-set methods [23]. See, as well, [14]. It relies on solving (2) by finite differences for the spatial derivatives and explicit Euler for time-stepping. Several variants were proposed over the years that use higher-order schemes for approximating the spatial derivatives or for time-stepping. A related approach is the Fast Marching Method of Sethian [19]. All these approaches rely on sampling the function and its derivatives on a grid (generally a regular grid, but methods working on hierarchical grids exist as well).

Deep neural networks for computational science While deep neural networks were originally designed for tackling problems of regression or classification, their use has now been extended to deal with different sorts of problems in computational sciences and applications.

Deep neural networks can be trained for computing the SDF to a given point-cloud or triangle mesh [1, 2, 3, 7, 11, 9, 22, 21, 24]. All these methods differ in how they model the loss function or the network architecture. For example, [22] proposes to use $\sin(\cdot)$ activation functions.

In this work, instead of starting from a point-cloud or a polygonal mesh, we assume that the input is a function f whose zero-level set describes the surface of interest. Information about the surface is embedded in the neural network by multiplying the final layer by the function f itself (or by a

smoothed version of $\text{sign}(f)$).

Related to our approach are recent techniques for solving Partial Differential Equations (PDE), including high-dimensional and stochastic PDE, [25, 6] with deep neural networks.

3 Approach

Given a function f whose zero level-set defines a surface S , our goal is to compute d , the signed distance to S (1). We look for the distance function d under the form

$$d(\mathbf{x}; \boldsymbol{\theta}) = f(\mathbf{x})g(\mathbf{x}; \boldsymbol{\theta}) \quad (3)$$

where g is a parametric function with parameters $\boldsymbol{\theta}$. We use a fully connected feedforward neural network for g . For fitting $\boldsymbol{\theta}$, the parameters of g , we express d as the solution to a variational problem (See Sections 3.2 and 3.3). An alternative to (3) is to use

$$d(\mathbf{x}; \boldsymbol{\theta}) = \text{sign}(f(\mathbf{x}))g(\mathbf{x}; \boldsymbol{\theta}), \quad (4)$$

where $\text{sign}(x)$ is a smoothed version of the sign function. For example, one can use $\text{sign}(x) \equiv \tanh(\alpha x)$, where α is a user-specified parameter.

3.1 Feedforward neural network

We use as an ansatz for $d(\mathbf{x})$, $f(\mathbf{x})g(\mathbf{x}; \boldsymbol{\theta})$, where $x_L = g(\mathbf{x}; \boldsymbol{\theta})$ is a deep, fully connected neural network defined by

$$\begin{aligned} x_L &= W_L \sigma(\mathbf{x}_{L-1}) + b_L \\ &\dots \\ \mathbf{x}_2 &= W_2 \sigma(\mathbf{x}_1) + b_2 \\ \mathbf{x}_1 &= W_1 \mathbf{x} + b_1. \end{aligned}$$

L corresponds to the number of layers in the deep neural network, W_i and b_i correspond to the parameters $\boldsymbol{\theta}$ of the neural network, and $\sigma()$ is a non-linear activation function.

3.2 Variational problems

The distance function d (1) is the viscosity solution to the eikonal equation [8]

$$|\nabla_{\mathbf{x}} d| = 1 \quad (5)$$

with boundary condition $d(\mathbf{x}) = 0$ for $\mathbf{x} \in S$. See, e.g. [5, 4] for recent numerical techniques to solve (5).

An alternative approach consists in considering the following p -Poisson problem

$$\Delta_p u = -1, \tag{6}$$

subject to $u = 0$ on S , and, where $\Delta_p u \equiv \operatorname{div}(|\nabla_{\mathbf{x}} u|^{p-2} \nabla_{\mathbf{x}} u)$ is the p -Laplacian.

Let u_p be the solution to (6), $u_p(\mathbf{x}) \rightarrow \operatorname{dist}(\mathbf{x}, S)$ as $p \rightarrow \infty$ and thus can be used to approximate the signed distance function to S [5, 10].

For a fixed value of p , the solution u_p to (6) only delivers an approximation of the distance function to S . The approximation quality can be improved by a simple normalization scheme as described in [5].

3.3 Loss functions

Let $g(\mathbf{x}; \boldsymbol{\theta} = (\mathbf{W}, _))$ be a deep, fully connected neural network with parameters $\boldsymbol{\theta} = (\mathbf{W}, _)$. We use the ansatz $d(\mathbf{x}; \boldsymbol{\theta}) = f(\mathbf{x})g(\mathbf{x}; \boldsymbol{\theta})$ (or $d(\mathbf{x}; \boldsymbol{\theta}) = \operatorname{sign}(f(\mathbf{x}))g(\mathbf{x}; \boldsymbol{\theta})$) for the distance function, where the parameters $\boldsymbol{\theta}$ need to be fitted.

Given that the distance function is the viscosity solution to the eikonal equation (5), we consider the following loss function (to be minimized)

$$L(\boldsymbol{\theta}) = \mathbb{E}_{\mathbf{x} \sim D} (|\nabla_{\mathbf{x}} d(\mathbf{x}; \boldsymbol{\theta})| - 1)^2, \tag{7}$$

where \mathbb{E} is the expected value, and D is the uniform distribution over the given computational domain.

Similarly, if one wants to solve the p -Poisson problem (6) instead, the correspond loss function is given by

$$L(\boldsymbol{\theta}) = \mathbb{E}_{\mathbf{x} \sim D} (\Delta_p d(\mathbf{x}; \boldsymbol{\theta}) + 1)^2. \tag{8}$$

It is possible to add other constraints to the loss (7) or the loss (8). For example, if necessary, one could prevent eventual extra zero level-sets away from the surface by adding a term such as

$$\mathbb{1}_{\{\mathbf{x}: f(\mathbf{x}) \neq 0\}} \exp(-\gamma |d(\mathbf{x}; \boldsymbol{\theta})|), \tag{9}$$

where $\mathbb{1}_X$ is the indicator function for the set X , and γ is a large value (for example $\gamma = 10^2$).

Stochastic Gradient Descent [18] or a variant, such as e.g. ADAM [12], is used for minimizing the loss function (7) or the loss function (8), with

eventual additional constraints such as (9).

The corresponding minimizer $d(\mathbf{x}; \boldsymbol{\theta} = \tilde{\boldsymbol{\theta}})$, with fitted parameters $\tilde{\boldsymbol{\theta}}$ provides the SDF to S (or an approximation in the case of (8)), while preserving exactly the zero level-set of f .

3.4 Derivatives computation

We rely on automatic differentiation to compute the spatial derivatives $\nabla_{\mathbf{x}}$, div , or Δ_p exactly. Note that the derivatives are taken here w.r.t. the input \mathbf{x} of the function.

For training the deep neural network, we also need to compute the derivatives of the loss functions (7) or (8) w.r.t. the parameters $\boldsymbol{\theta} = (\mathbf{W}, _)$. This is also performed by automatic differentiation as usually done when training deep neural networks.

4 Numerical results

4.1 Setup

We use Torch [17] for specifying the deep neural network, computing the derivatives (w.r.t. the network’s parameters and the coordinates), and minimizing the loss function.

For the network g we use 8 fully connected linear layers with width 512. We use a skip connection from the input to the middle layer. The architecture is similar to the one described in [15] and in [11].

The softplus activation function is used for the non-linear activation functions

$$\sigma(x) = \frac{1}{\beta} \ln(1 + \exp(\beta x)).$$

We used $\beta = 100$ in the experiments. Using the softplus activation function behaved better in our experiments than the Rectified Linear Unit (RELU), which is typically used with deep neural networks. Note that it is also possible to consider alternatives such as the SIREN layer [22] for the activation function. We did not experiment with this alternative.

In the final layer, we multiply the output of the neural network $g(\mathbf{x}; \boldsymbol{\theta})$ by $\tanh(\alpha f(\mathbf{x}))$, the smoothed sign function of $f(\mathbf{x})$. We used $\alpha = 0.1$.

We minimize the loss function (7) (or (8)) by ADAM [12], using a learning rate of 0.0001. The parameters of the neural network are initialized with the geometric initialization of [2].

For the computation of the loss functions (7) or (8), we use the uniform distribution over the computational domain for the distribution D .

4.2 Results

4.2.1 1D example

We start our numerical experiments with a simple example in 1D: We consider the domain $[0, 1]$ with boundary the points $\{0, 1\}$. We build an implicit for this domain as

$$f(x) = x + (1 - x) + \sqrt{x^2 + (1 - x)^2},$$

i.e. the intersection of the half-spaces x and $(1 - x)$ with the intersection implemented by an R-function [20, 16].

Note that in this case, the exact SDF to the boundary is known and is given, of course, by

$$\min(x, 1 - x).$$

Figure 1 shows a plot of the function f (top-left image), the distance computed by solving the eikonal equation (5) in the top-right image, and the approximate distance obtained by solving the p -Poisson problem (6) with $p = 2, 8$, respectively (bottom left and right images).

Solving (5) or (6) is done by minimizing the corresponding loss function (7) or (8), respectively. We used 15000 iterations in both cases.

To verify the quality of the solutions, we also show in Fig. 2 the distribution of the p -Laplacian $\Delta_p d(\mathbf{x})$, $p = 2, 8$, for the solution to (6), in the left and middle images, and the norm of the gradient $|\nabla_{\mathbf{x}} d(\mathbf{x})|$, for the solution to (5), in the right image. Notice how the distributions are centered around -1 for the solution to the p -Poisson problem, and around 1 for the solution to the eikonal equation.

4.2.2 2D example

In 2D, we consider the function

$$f(x, y) = 1 - x^2 - y^2,$$

whose zero level-set correspond to a unit circle.

The exact SDF to the unit circle is, of course, known and given by

$$1 - \sqrt{x^2 + y^2}.$$

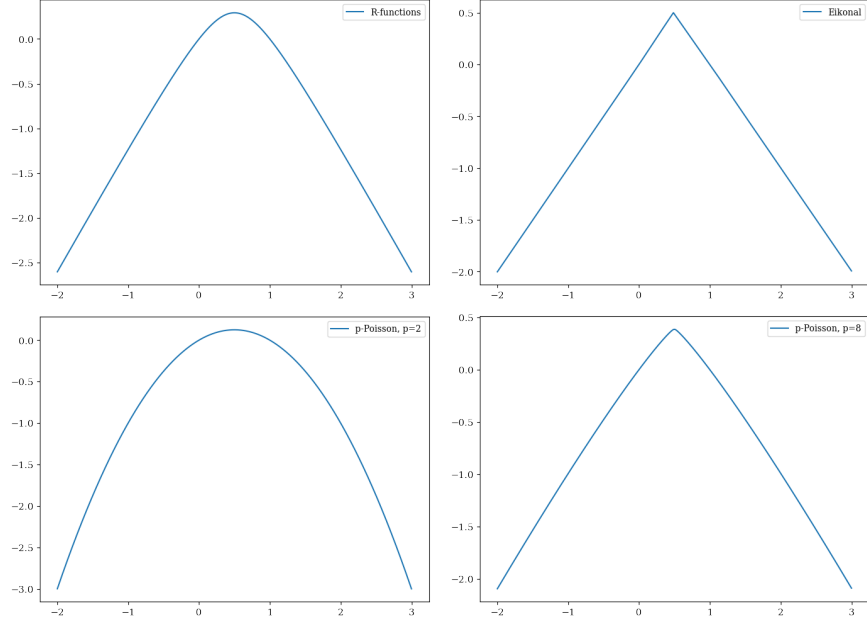


Figure 1: Results in 1D. Top row: Plot of $f(x) = x + (1-x) + \sqrt{x^2 + (1-x)^2}$ (left image); Minimizing (7), right image. And minimizing (8) with $p = 2$, $p = 8$ (left and right, respectively) in the bottom row. Note that the zero level-set of f (the points $\{0, 1\}$) is exactly preserved.

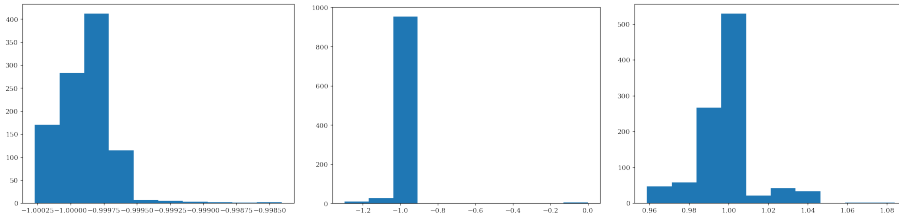


Figure 2: Left: Distribution of the values of the Laplacian Δd ($\Delta_p d$ with $p = 2$). Middle: Distribution of the values of the p -Laplacian $\Delta_p d$, $p = 8$. Right: Distribution of the values of $|\nabla d|$. The computational domain is the interval $[-2, 3]$. The values are centered around -1 for $\Delta_p d$ and 1 for $|\nabla d|$.

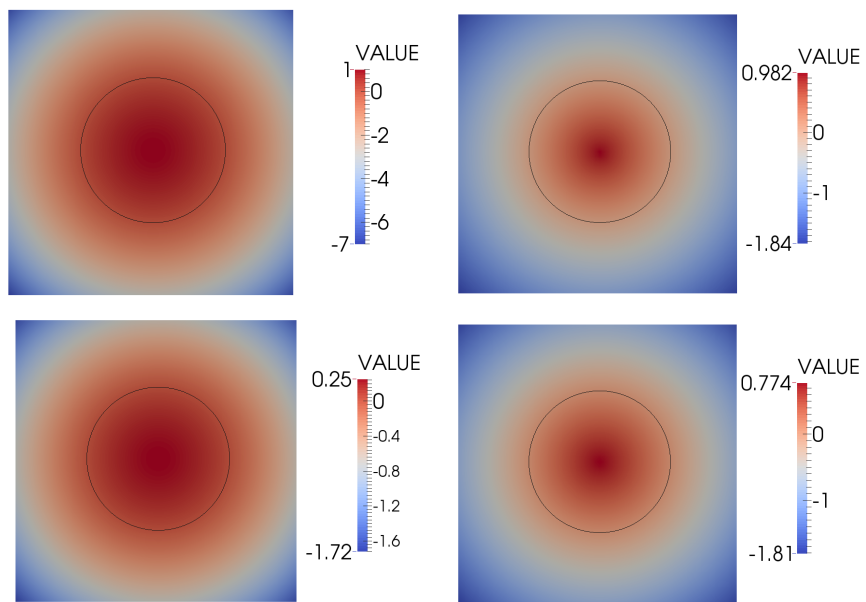


Figure 3: Top row: Filled contour plot of $f(x, y) = 1 - x^2 - y^2$ (left). Right image: SDF obtained by minimizing the loss (7). Bottom row: Approximate SDF obtained by minimizing (8) for $p = 2$ (left) and $p = 8$ (right). Note how the zero level-set of f is exactly preserved in all cases.

Figure 3 illustrate the results obtained by our approach. The top row shows filled contour plots for the input function $f(x, y)$ and the solution to the eikonal equation (5) obtained by minimizing (7). The bottom row show the solution to the p -Poisson problem for $p = 2$ (left) and $p = 8$ (right), respectively. In all cases, we used 15000 iterations of ADAM. Notice again how the zero level-set of f is exactly preserved.

4.2.3 3D example

We use a more complex model to illustrate our approach in 3D. See the left image in Fig. 4. This object is built from "algebraic" primitives (a sphere, a

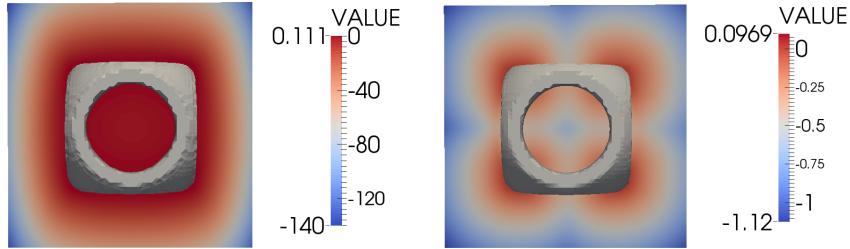


Figure 4: Zero level-set and filled contour plot on a slice for the original implicit (left) and the SDF obtained by minimizing the loss (7).

box and three cylinders), and CSG operations implemented by R-functions [16]. The term "algebraic" refers here to the fact that we are not using distance-based primitives. For example, we use

$$1 - x^2 - y^2 - z^2,$$

and

$$1 - x^2 - y^2$$

for a sphere and a cylinder, respectively.

Figure 4, left image, shows with a filled contour plot on a given slice of the object that the function f defining the object does not correspond to the distance to the surface S .

Figure 4, right image, shows the solution to (5). It corresponds to the deep neural network obtained from minimizing the loss function (7). We used 15000 iterations of ADAM (similar to the 1D and 2D examples). Notice how the solution delivers a good approximation of the signed distance to

the surface. Since the original implicit f is embedded in the last layer of the deep neural network, the zero level-set of f is exactly preserved.

5 Conclusion

We proposed in this short note a technique for re-distancing an implicit surface. Given a function f whose zero level-set defines a geometric surface S , we want to compute the signed distance to S (or an approximation), while preserving exactly the zero level-set of f . We do that by embedding the function f in the last layer of a deep neural network, which is then trained on a loss function derived from an eikonal equation. Alternatively, we propose a different loss function corresponding to the p -Poisson problem $\Delta_p u = -1$, whose solution delivers an approximation to the distance function.

References

- [1] Matan Atzmon, Niv Haim, Lior Yariv, Ofer Israelov, Haggai Maron, and Yaron Lipman. Controlling neural level sets. *arXiv preprint arXiv:1905.11911*, 2019.
- [2] Matan Atzmon and Yaron Lipman. SAL: Sign agnostic learning of shapes from raw data. In *Proceedings of the IEEE/CVF Conference on Computer Vision and Pattern Recognition*, pages 2565–2574, 2020.
- [3] Matan Atzmon and Yaron Lipman. SAL++: Sign agnostic learning with derivatives. *ArXiv preprint arXiv:2006.05400v1*, 2020.
- [4] Alexander Belyaev and Pierre-Alain Fayolle. An admm-based scheme for distance function approximation. *Numerical Algorithms*, pages 1–14, 2019.
- [5] Alexander G Belyaev and Pierre-Alain Fayolle. On variational and pde-based distance function approximations. *Computer Graphics Forum*, 34(8):104–118, 2015.
- [6] Jan Blechschmidt and Oliver G Ernst. Three ways to solve partial differential equations with neural networks—a review. *ArXiv preprint arXiv:2102.11802*, 2021.
- [7] Julian Chibane, Aymen Mir, and Gerard Pons-Moll. Neural unsigned distance fields for implicit function learning. *ArXiv preprint arXiv:2010.13938*, 2020.

- [8] Michael G Crandall and Pierre-Louis Lions. Viscosity solutions of hamilton-jacobi equations. *Transactions of the American mathematical society*, 277(1):1–42, 1983.
- [9] Thomas Davies, Derek Nowrouzezahrai, and Alec Jacobson. On the effectiveness of weight-encoded neural implicit 3d shapes. *ArXiv preprint arXiv:2009.09808 [cs.GR]*, 2021.
- [10] Pierre-Alain Fayolle and Alexander G Belyaev. p -Laplace diffusion for distance function estimation, optimal transport approximation, and image enhancement. *Computer Aided Geometric Design*, 67:1–20, 2018.
- [11] Amos Gropp, Lior Yariv, Niv Haim, Matan Atzmon, and Yaron Lipman. Implicit geometric regularization for learning shapes. *ArXiv preprint arXiv:2002.10099*, 2020.
- [12] Diederik P Kingma and Jimmy Ba. Adam: A method for stochastic optimization. *ArXiv preprint arXiv:1412.6980*, 2014.
- [13] William E Lorensen and Harvey E Cline. Marching cubes: A high resolution 3d surface construction algorithm. *ACM siggraph computer graphics*, 21(4):163–169, 1987.
- [14] Stanley Osher and Ronald Fedkiw. *Level set methods and dynamic implicit surfaces*, volume 153. Springer Science & Business Media, 2006.
- [15] Jeong Joon Park, Peter Florence, Julian Straub, Richard Newcombe, and Steven Lovegrove. DeepSDF: Learning continuous signed distance functions for shape representation. In *Proceedings of the IEEE/CVF Conference on Computer Vision and Pattern Recognition*, pages 165–174, 2019.
- [16] Alexander Pasko, Valery Adzhiev, Alexei Sourin, and Vladimir Savchenko. Function representation in geometric modeling: concepts, implementation and applications. *The visual computer*, 11(8):429–446, 1995.
- [17] Adam Paszke, Sam Gross, Francisco Massa, Adam Lerer, James Bradbury, Gregory Chanan, Trevor Killeen, Zeming Lin, Natalia Gimelshein, Luca Antiga, Alban Desmaison, Andreas Kopf, Edward Yang, Zachary DeVito, Martin Raison, Alykhan Tejani, Sasank Chilamkurthy, Benoit Steiner, Lu Fang, Junjie Bai, and Soumith Chintala. Pytorch: An imperative style, high-performance deep learning library. In H. Wallach,

- H. Larochelle, A. Beygelzimer, F. d'Alché-Buc, E. Fox, and R. Garnett, editors, *Advances in Neural Information Processing Systems 32*, pages 8024–8035. Curran Associates, Inc., 2019.
- [18] Herbert Robbins and Sutton Monro. A stochastic approximation method. *The annals of mathematical statistics*, pages 400–407, 1951.
- [19] James A Sethian. A fast marching level set method for monotonically advancing fronts. *Proceedings of the National Academy of Sciences*, 93(4):1591–1595, 1996.
- [20] Vadim Shapiro. Semi-analytic geometry. *Acta Numerica 2007: Volume 16*, 16:239–303, 2007.
- [21] Vincent Sitzmann, Eric R Chan, Richard Tucker, Noah Snavely, and Gordon Wetzstein. Metasdf: Meta-learning signed distance functions. *ArXiv preprint arXiv:2006.09662*, 2020.
- [22] Vincent Sitzmann, Julien Martel, Alexander Bergman, David Lindell, and Gordon Wetzstein. Implicit neural representations with periodic activation functions. *Advances in Neural Information Processing Systems*, 33, 2020.
- [23] Mark Sussman, Peter Smereka, and Stanley Osher. A level set approach for computing solutions to incompressible two-phase flow. *Journal of Computational physics*, 114(1):146–159, 1994.
- [24] Towaki Takikawa, Joey Litalien, Kangxue Yin, Karsten Kreis, Charles Loop, Derek Nowrouzezahrai, Alec Jacobson, Morgan McGuire, and Sanja Fidler. Neural geometric level of detail: Real-time rendering with implicit 3D shapes. *ArXiv preprint arXiv:2101.10994*, 2021.
- [25] E Weinan and Bing Yu. The deep ritz method: a deep learning-based numerical algorithm for solving variational problems. *Communications in Mathematics and Statistics*, 6(1):1–12, 2018.